2D RADIATION SHOCK BREAKOUT OF RSG WITH CSM

Wun-Yi Chen[1,2], Ke-Jung Chen[1], Masaomi Ono[1,3], Po-Sheng Ou[1,2]

[1]Academia Sinica, Institute of Astronomy and Astrophysics

[2]National Taiwan University, Graduate Institute of Astrophysics

[3]Astrophysical Big Bang Laboratory, RIKEN Cluster for Pioneering Research

ABSTRACT

We present new multidimensional radiation simulations of a $20\,M_{\odot}$ RSG shock breakout with the CASTRO code. Shock breakout signal can provide progenitors information and pre-explosion environment with its extreme luminosity and short duration. Detailed opacity from OPAL with Multi-Group Flux-Limited Diffusion provide double luminosity peaks on band from infrared ray to X-ray. We perform constant mass loss rate CSM across 2 orders of magnitude. This work is a great extension from SN1987a of P2-AG-022 to RSG progenitors.

INTRODUCTION

The electromagnetic signals from supernovae (SNe) of massive stars begin when the explosion shock breaks out of the stellar surface*. The so-called shock breakout offer crucial insights into explosion energy, progenitor star radius, and circumstellar environment (CSM) with the observed luminosity light curves (LCs) and shock duration**. Previous models in 1D simulations fell short and create thin shell near the shock front, necessitating the shift to 2D simulations*. Recent 2D rad-hydros simulations* can not evaluate heating and cooling of X-ray and UV emissions with grey opacity. Our research presents the **first results** of multidimensional multi-group rad-hydros simulations on red supergiants (RSGs). We focus on a $20\,M_{\odot}$ star* and compare observables of different CSM calculated from constant mass loss rates across two orders of magnitude. The progenitor is around 40 times larger than the BSGs, having significant denser CSM that generate longer shock duration and dimmer peak luminosity. We employ 2D Multi-Group Flux Limited Diffusion (MGFLD) in **CASTRO*** and incorporating **OPAL** opacity tables*.

METHODOLOGY

1. **CASTRO:** After explosion shock reaching stellar surface in **FLASH***, the progenitor is transferred to **CASTRO**, a compressible rad-hydros code. Employing 2D cylindrical box with $10^{15}\,\mathrm{cm}$ and 1024 grids each side, reflective and outflow are applied to the lower and upper boundaries, respectively. We use γ law equation of state with poisson gravity.
2. **Rad-Hydro:** MGFLD govern interaction between radiation flux and opacity. We choose 8 radiation groups covering 10^5 to $1\,\mathrm{\AA}$ (infrared ray to X-ray) and calculate opacity from **OPAL** by separating partial degenerate electron scattering*, free-free, and bound-free opacity ($\kappa \propto T^{0.5}\nu^{-3}$). We calculate LCs with different wavelength λ and viewing angles θ by $L_{\lambda,\theta} = 4\pi r^2 F_{\lambda,\theta}$.
3. **Stellar Surface and CSM:** We derived CSM from constant mass loss rate of $\alpha\dot{M} \sim 6.46\times10^{-6}\,M_{\odot}\,\mathrm{yr}^{-1}$ with α covering 2 orders of magnitude and wind velocity of $3\times10^{6}\,\mathrm{cm\,s^{-1}}$.

RESULTS

1. **Structures:** We demonstrate structures formation of explosion shock colliding with dense CSM that enhance both the **Rayleigh-Taylor** instabilities and **reverse shock**. (Fig. 1) The shock wave propagates and collide with CSM, create inverse gradient of density and radiation pressure. Due to dense environment, there are multiple-layers such that initial reverse shock propagates back and hinder the secondary shock regions. IN the light CSM, the reverse shock and Rayleigh-Taylor instabilities are not evident. (Fig.2)
2. **LCs:** Calculate LCs across wavelengths offer spectral energy distribution and show **double peaks** for each wavelengths. (Fig. 3) Resulting LCs of X-Ray and UV radiation flux are vital for observation strategies, the post-breakout luminosity decline rate and offer indicators for shock breakout tail.

1

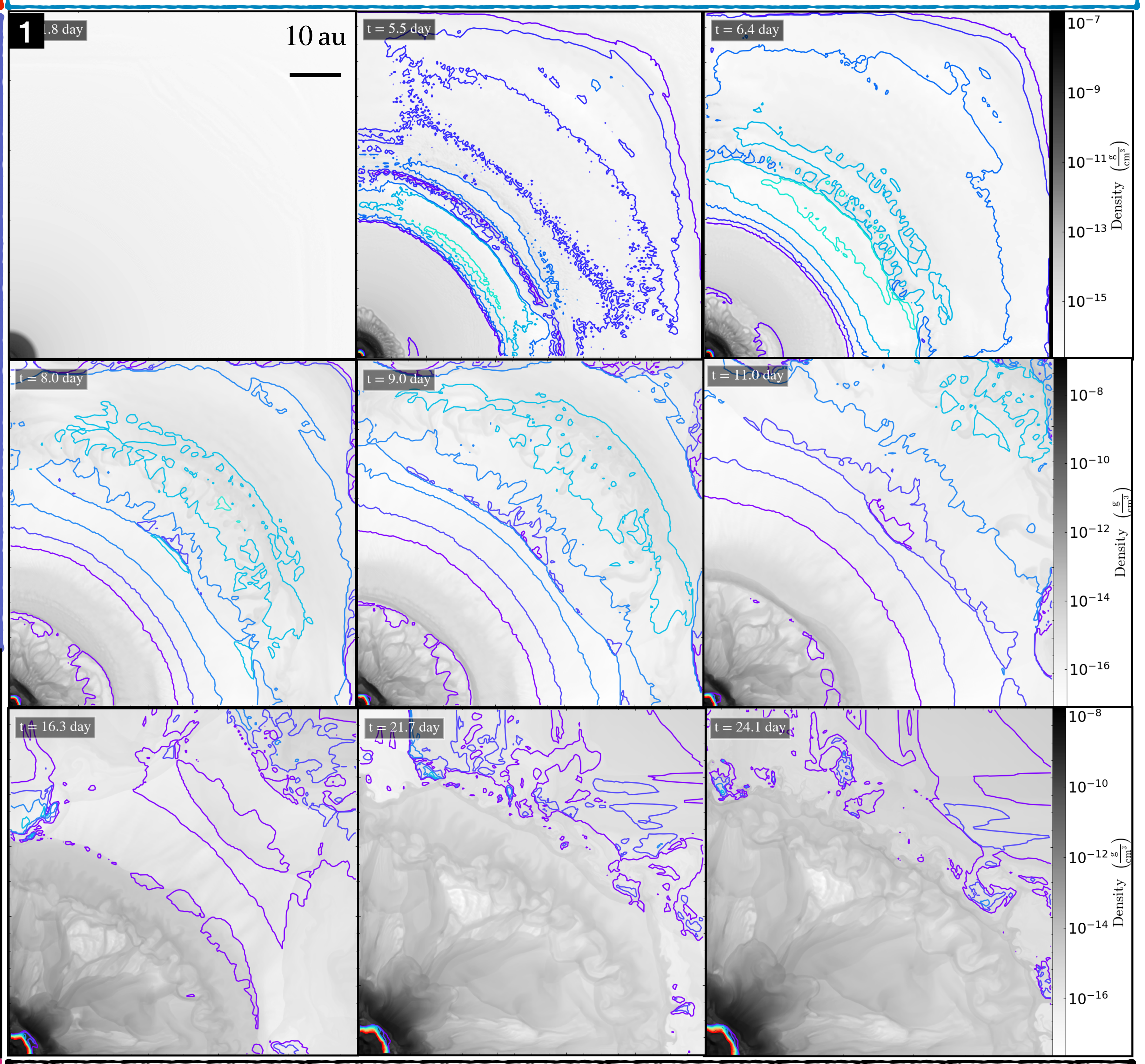

2

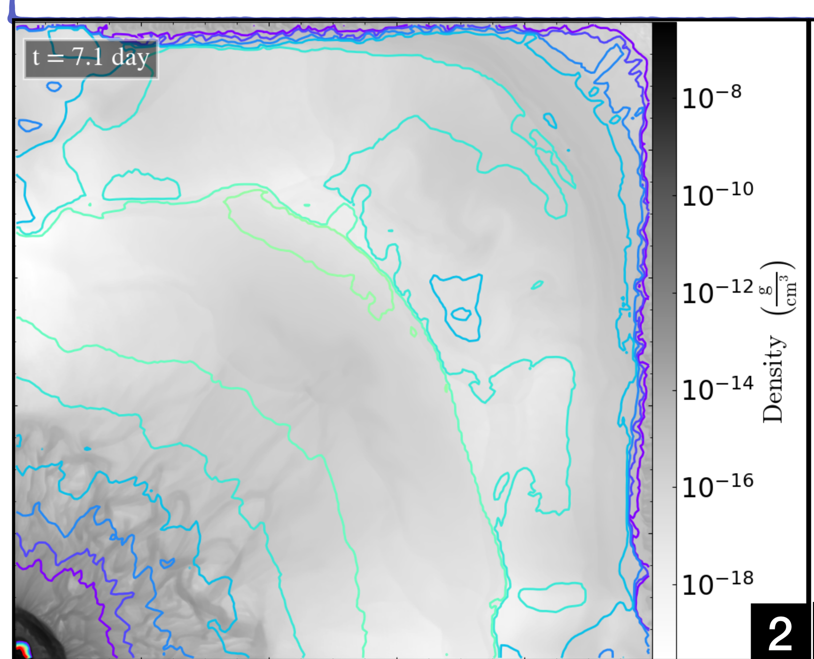

3

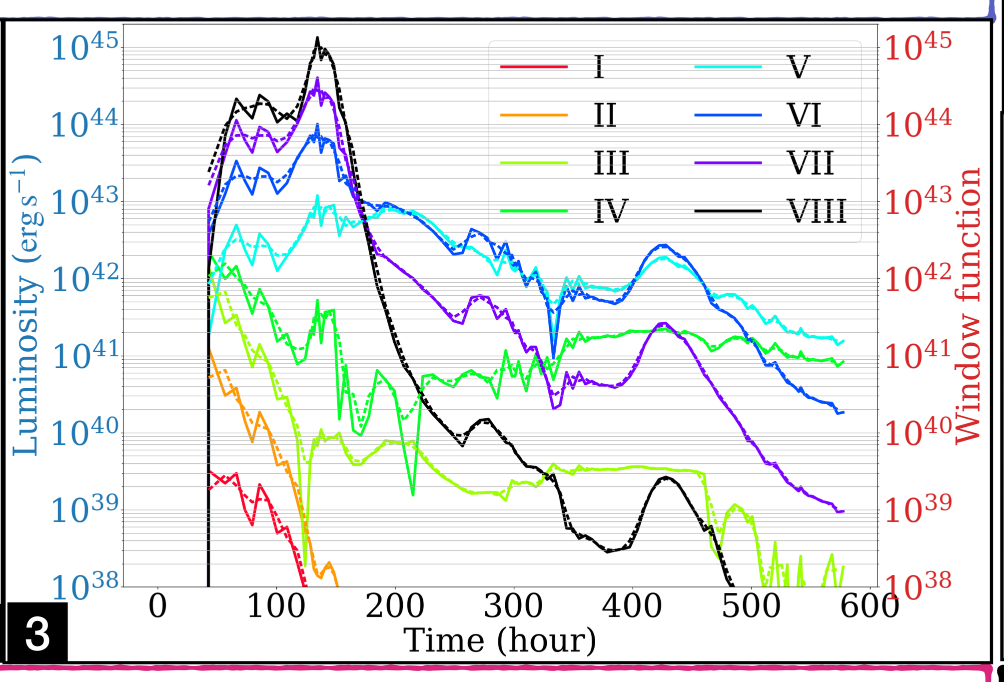

CONCLUSION

1. **2D simulations:** We have extended shock duration due to 2D fluid mixing, in stead of the dense envelopes required in 1D simulations*. The post-breakout luminosity decline rate for X-ray is up to $\dot{L} \sim 4\,\mathrm{mag\,day^{-1}}$ while for UV band is $\dot{L} \sim 0.8\,\mathrm{mag\,day^{-1}}$, so the dominant band transit to UV a day after the peak luminosity. The system have the second peak at 450 hours after the breakout, and are found to have $\dot{L} \sim 0.6\,\mathrm{mag\,day^{-1}}$ afterwards.
2. **Colored Opacity:** Provide spectral energy distribution and cooling process in LCs, we discovered that shock breakout is sensitive to pre-explosion environment and can provide information of motion in stellar envelopes, late-time stellar evolution , and binary systems.

This research is supported by MOST 110-2112-M-001-068-MY3 and AS-CDA-111-M04. Our computing resources were supported by the National Energy Research Scientific Computing Center (NERSC) and the TIARA Cluster at the Academia Sinica Institute of Astronomy and Astrophysics (ASIAA).

REFERENCE

*Waxman, E., & Katz, B. 2017, in Handbook of Supernovae, ed. A. W. Alsabti & P. Murdin, 967, doi: 10.1007/978-3-319-21846-5 33

*Schawinski, K., Justham, S., Wolf, C., et al. 2008, Science, 321, 223, doi: 10.1126/science.1160456

*Gezari, S., Jones, D. O., Sanders, N. E., et al. 2015, ApJ, 804, 28, doi: 10.1088/0004-637X/804/1/28

*Lovegrove, E., Woosley, S. E., & Zhang, W. 2017, ApJ, 845, 103, doi: 10.3847/1538-4357/aa7b7d

*Suzuki, A., Maeda, K., & Shigeyama, T. 2016, Astrophysical Journal, 825, doi: 10.3847/0004-637X/825/2/92

*Ou, P.-S., Chen, K.-J., Chu, Y.-H., & Tsai, S.-H. 2023, The Astrophysical Journal, 944, 34,doi: 10.3847/1538-4357/aca96e

*Almgren, A., Sazo, M. B., Bell, J., et al. 2020, Journal of Open Source Software, 5, 2513, doi: 10.21105/joss.02513

*Iglesias, C. A., & Rogers, F. J. 1996, ApJ, 464, 943, doi: 10.1086/177381

*Buchler, J. R., & Yueh, W. R. 1976, ApJ, 210, 440, doi: 10.1086/154847

*Hiramatsu, D., Tsuna, D., Berger, E., et al. 2023, The Astrophysical Journal Letters, 955, L8,doi: 10.3847/2041-8213/acf299